Engineered Science
DOI: https://dx.doi.org/10.30919/es1440

Mathematical Modeling for Virus Immunization and Vaccination

Ashish Kumar,[1] Dinesh Kumar Saini[2,*] and Yerra Shankar Rao[3]

Abstract

A global pandemic, COVID-19, broke out in 2020, causing an emergency. The whole world was in deep trouble, which forced the entire world to go into lockdown, prompting a worldwide effort to develop vaccines. By then, several countries, including the USA, UK, Russia, India, China, and Israel, started producing a range of vaccines to combat the virus. The vaccination drive started vaccinating vulnerable populations, including older adults and individuals with underlying health conditions. The efficacy and effectiveness of these developed vaccines vary from vaccine to vaccine, and there is a need to calculate the efficacy of each developed vaccine. The effectiveness of these vaccination campaigns can be modeled mathematically using differential equations to simulate population dynamics, helping to predict when herd immunity might be achieved. The vaccination drive helped in controlling this pandemic, and a mathematical model helped us identify potential threats emerging from new variants of the coronavirus. Getting full immunity in the population and herd immunity is very difficult, but efforts are made to predict. COVID-19 deaths can be mitigated if a vaccination scenario is modeled using the SVIR (susceptible, vaccinated, infected, and recovered). Simulation results show that vaccination and timing have an impact on the total population for achieving herd immunity.

Keywords: Vaccination; COVID-19; SVIR; Immunity; Basic reproduction number; Susceptibility; Sustainability; Optimization.
Received: 25 November 2024; Revised: 31 January 2025; Accepted: 22 February 2024.
Article type: Research article.

1. Introduction

Malicious objects like viruses, bacteria, and fungi create infectious diseases and take millions of lives worldwide. Vaccination is one of the solutions that evolved over years of research, but measuring the effectiveness of these vaccines is still a matter of concern. The virus that emerged in 2019 has since caused a global outbreak, and to this day, the world continues to experience the profound impacts of COVID-19 on human life. The World Health Organization (WHO) has classified COVID-19 as a globally hazardous disease. During this period, the exponential spread of this virus has been experienced, which makes it most hazardous. Various steps are being taken, such as lockdowns and vaccination drives. But this was just a short-term solution with low accuracy, which has reduced the spread, but the rate at which the population needs to be made immune is slow and time-consuming. There have been various other viruses in the past, like Human Immunodeficiency virus (HIV), Tuberculosis (TB), and many more, but the vaccine designed for them is more effective than existing vaccines for COVID-19.

Testing, treatments, and vaccination are the three main tasks that were initiated. During the COVID-19 pandemic, many companies have worked on various types of solutions to cure and vaccines to make humans immune to this disease. However, due to the early stages of the vaccines and less testing, the efficacy of the vaccines is very low. Thus, the efficacy of vaccines varies from age group and type of environment or the health condition of the people. For example, the same vaccine that has high efficacy in Asia turns out to be low in other continents. Therefore, to determine the immunity of the total population, this study has been performed to estimate the time required to vaccinate and generate immunity over the total population. The work is based on the WHO database available online for various countries. The work uses the data available on the WHO web portal for the study.

[1] *Department of Mathematics & Statistics, Manipal University Jaipur, Jaipur, Rajasthan, 303007, India*
[2] *Department of IoT and Intelligent Systems, Manipal University Jaipur, Jaipur, Rajasthan, 303007, India*
[3] *Department of Mathematics, NIST University, Berhampur, Odisha, 761008, India*
**Email:* dineshkumar.saini@jaipur.manipal.edu (D. K. Saini)

Vaccination will reduce the deaths caused by malicious objects like viruses, worms, and fungi. In this paper, we are formulating a mathematical model for the effect of vaccination on the total population. Vaccination will prove to be a game-changer. The duration to get vaccinated and to get herd immunity was very difficult to predict. The efficacy and effectiveness of these vaccines also vary. The problems addressed in the paper address these four major questions, which are as follows.

Q1: Identification of the best COVID-19 spread model that suits the Indian scenario. Is vaccination effective in mitigating death rates?

Q2: Mortality and morbidity rates in various groups who got vaccinated with one dose and a second dose.

Q3: Period of vaccination and how much time it will take to acquire herd immunity, taking into account the efficacy of the vaccines by different vendors.

Q4: Do the 45+ age group and 18+ age group affect susceptible people?

2. Related work

Vaccination helps in establishing herd immunity, reduces the spread, and creates protection. Despite their proven success, vaccines have faced challenges, including misinformation, vaccine hesitancy, and unequal access, highlighting the need for continued education, research, and global collaboration. In this section, some of the latest work in the field of existing models for prediction in various pandemics is discussed, which are referred to in our work. The work also showcases existing approaches proposed for COVID-19 behaviour prediction and analysis.

Pinter proposed a machine-learning model for the prediction of the spread of the COVID-19 virus in Hungary for 2020.[1] The author has showcased a study on the existing situation in Hungary based on the data on the number of cases and mortality. Based on the existing data, the author has proposed a hybrid model using multiple optimization models. In this approach, they have proposed a multi-layered neural network and an International Cooperative Alliance (ICA)-based approach for complex datasets. The model is able to predict the peak of COVID with an accuracy of 96%.

Amit *et al*.[2] proposed a Gaussian-based model for the prediction of COVID-19 future cases. The author has tested the proposed model with the active number of cases in India, Italy, and the USA. The work was able to predict the future number of active cases for the next 7-28 days for all three countries with a high accuracy of 95%. The model fits the active dataset and predicts the date for the end of the peak of COVID-19 in India, Italy, and the USA, irrespective of the new variant and vaccination rate.

Study on various computational techniques for the detection of COVID-19 symptoms using x-ray imaging, health conditions, Computational Biology and Medicines, and Awareness and social control, the study of various work in each field of COVID-19 prevention.[3] In Wang *et al.* (2021),[4] Narin *et al.* (2021),[5] Wang *et al.* (2020),[6] Koucha *et al*. (2021),[7] and Xu *et al.* (2019),[8] various approaches for COVID prediction in check computed tomography (CT) scan images are proposed using deep learning, deep convolutional neural network, and recurrent neural network. The work showcased in their work is based on the COVID prediction based on the lunch condition, which defines the stage of infection. The work also proposed improvements in each work as compared to others.[4-8]

There are works that we summarized in the table below in prediction modelling. Rath *et al*.(2020) have proposed a model to predict the COVID spread, and the maximum peak in Odisha is shown using a multiple linear regression model. The work showcases a model to predict the maximum number of cases and the duration of the peak COVID-19 in Odisha. However, the model only takes into account the spread rate and the time-bound a patient can be treated, which restricts the coverage of the model and makes it generalized for the other zones in India and around the world.[9]

Other than the above studies, there have been various other works to study the behaviours of the COVID-19 spread and recovery. But in the past susceptible, infected, recovered (SIR) model has been used to predict the behaviour of various pandemic and vaccination campaigns like torulosis, H1N1, SAR, and many more. Some of such works listed below have referred to various prediction models that are used to predict the timeline of COVID-19. In this work, they have cited the work from mathematical models, the Autoregressive model, and the Exponential model.[10,11]

There exist various models to study the behaviors of systems and predict future performance. Given below are some categories of models to study the behavior. Ahmar *et al*.,[12] Al-Qaness *et al*.,[13] Chintalapudi *et al*.,[14] Chaudhry *et al*.,[15] Moftakhar and Mozhgan,[16] Chen *et al*.,[17] Chimmula and Zhang,[18] and Calafiore *et al.*[19] proposed various mathematical, autoregressive, and exponential models, including SIR, susceptible, exposed, infected, recovered (SEIR), prophet algorithm, genetic programming, and susceptible, infected, recovered, deceased (SIRD).

The above-discussed models are being used for predicting various types of behaviour of COVID-19, such as spread, mortality rate, vaccination rate, recovery rate, and the time of the peak of COVID-19 under various scenarios. Calafiore *et al*. have proposed a SIRD model to predict the duration of COVID-19 in Italy with various other aspects like the peak time, and spread rate, keeping in mind the local environment of Italy, which plays an important role in predicting the behavior of a spread rather than just the data.[19] In this pandemic situation of COVID-19, since 2019, various countries have tried multiple ways to restrict the spread of the virus. The ways may be lockdown, social distancing, or even restrictions on travelling by air from one country to another. But these measures are just primary measures to avoid COVID-19, and vaccination is the most effective measure to overcome any pandemic situation. Ins this pandemic, many

companies rushed to provide a vaccine as early as possible with the least testing, which has led to low efficacy of the vaccine, even with variable effectiveness on variants of this virus. The vaccine development, which takes 2-3 years, was completed in less than 6 months. Due to this, this study focuses on the performance of the vaccination doses and their effect on the immunity of the population vaccinated. The work also identifies the count of the population that is vaccinated but still exposed to the virus due to low efficacy.

3. Proposed model

In this work, a model is proposed to study the effect of vaccination on COVID-19 control based on multiple parameters like vaccination rate and the efficacy of a vaccine that may be COVISHIELD. COVAXIN or any other, decay of vaccination effect, and mortality and morbidity rates. The study will allow the country to estimate the period in which the almost complete population will get vaccinated and become immune to the virus, taking into account various age groups and the efficacy of the various existing vaccines because every vaccine comes with its own accuracy and efficacy, which varies for each age group. The proposed model takes into account all such multiple variables in order to tune the mathematical model that best fits the existing scenario.

3.1 Model descriptions and formulations

A mathematical model is one of the most important tools used in understanding the dynamic behavior of the Corena Virus disease transmission. To control and prevent the spread of this disease, effective methods of vaccination are widely used. This proposed model indicates populations with unique mutually exclusive natures. We consider four mutually exclusive populations for the human population concerning the Corena virus disease status. These total human populations can be divided into four subpopulations: Susceptible (S), Vaccinated (V), Infected (I), and Recovered (R).

The susceptible population is made up of the population who are not yet infected but stand a chance of infection by contact with the infected population. The infected population is made up of individuals who have the full-blown infection with symptomatic evidence of the disease. The recovered population is made up of individuals who have either undergone treatment or a vaccination process and have fully recovered from the infection through immunity. The vaccinated population is made up of individuals who have undergone vaccine doses from different vaccinations.

3.2 Behaviour of the model and assumptions

The flow diagram of the model is depicted in Fig. 1 and described based on the following assumptions (1-9). The nomenclature of the mathematical model is appended in Table 1.

1. The susceptible population is increased by the recruitment rate (T)/ inflow of individuals in the region, either by birth or by immigration.
2. The natural death of each of the population is decreased by the constant 'μ_1'
3. The susceptible population moves to the vaccination given by the different administrations of anti-COVID-19 vaccines at the rate of 'r'.
4. The susceptible and vaccinated populations may acquire infection by contact with the infected population at the rate 'β'.
5. Since the vaccine is assumed to be imperfect, the proportion against the infection is not 100%, so the vaccinated population gets infected.
6. The efficacy of the vaccine is at the rate r. The effective contact rate β is multiplied by a scaling factor (1-r), where 0<r<1.
7. Newly infected people who developed clinical symptoms of COVID-19 disease are at a rate 'e'.
8. The symptomatic population is diminished by recovery at the rate 'γ'
9. The symptomatic population is induced by the death 'μ_2 '.

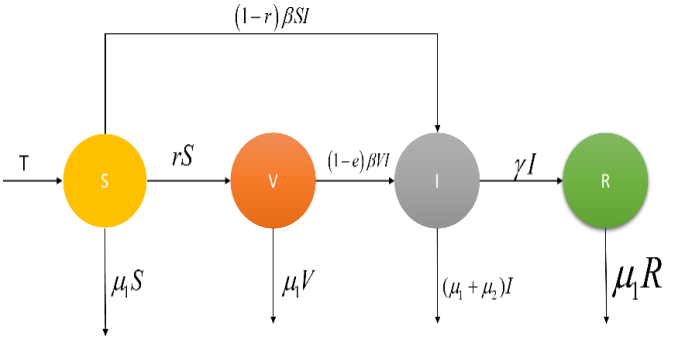

Fig. 1: Diagram of the model.

Table 1: Nomenclature.

Notations	Descriptions
S	Susceptible populations
V	Vaccinated population
I	Infected populations
R	Recovered populations
N	Total number of populations under consideration
T	Recruitment (birth or immigration) rate of susceptible Populations
β	Effective contact rate
r	Rate of coverage of vaccine
e	Efficacy of the vaccine
γ	Rate of recovery
μ_1	Natural mortality rate
μ_2	COVID-19-induced mortality rate

3.3 Mathematical model

The rate of change of the population in each subpopulation is represented by the following system of nonlinear ordinary differential Equations 1-4:

$$\frac{dS}{dt} = T - (1-r)\beta SI - rS - \mu_1 S \quad (1)$$

$$\frac{dV}{dt} = rS - (1-e)\beta VI - \mu_1 V \quad (2)$$

$$\frac{dI}{dt} = (1-r)\beta SI + (1-e)\beta VI - (\mu_1 + \mu_2 + \gamma)I \quad (3)$$

$$\frac{dR}{dt} = \gamma I - \mu_1 R \quad (4)$$

3.3.1 Model analysis

The positivity of the trajectories, combined with the boundedness of the total population, leads to the internal stability of the given model through analysis. This implies the boundedness of all subpopulations discussed**.**

3.3.2 Invariant region

In this section, we define the region where the solution to the model is uniformly bounded as the set of community $\Omega \in R_+^4$. The total number of nodes in the region is in Equation 5:

$$\text{de}\frac{dN}{dt} = \frac{dS}{dt} + \frac{dV}{dt} + \frac{dI}{dt} + \frac{dR}{dt}$$

$$\Rightarrow \frac{dN}{dt} = T - (1-r)\beta SI - rS - \mu_1 S + rS - (1-e)\beta VI - \mu_1 V + (1-r)\beta SI + (1-e)\beta VI - (\mu_1 + \mu_2 + \gamma)I + \gamma I - \mu_1 R$$

$$\Rightarrow \frac{dN}{dt} = T - N\mu_1 - \mu_2 I$$

$$\Rightarrow N = \frac{T-\mu_2 I}{\mu_1} \quad (5)$$

with $N = S + V + I + R$

It follows that $0 \le \lim_{t\to\infty} sup\, N(t) \le N_0$ with $\lim_{t\to\infty} sup\, N(t) = N_0$ iff $\lim_{t\to\infty} sup\, I(t) = 0$

Similarly, $0 \le \lim_{t\to\infty} sup\, S(t) \le S_0$

Again $0 \le \lim_{t\to\infty} sup\, V(t) \le V_0$

Hence, the above equation shows that $N > N_0 \Rightarrow \frac{dN}{dt} < 0$

This established the set $\Omega = \{(S,V,I,R) \in R_+^4 : S + V + I + R \le N_0; S \le S_0, V \le V_0\}$ is positive invariant in the transmission model.

This positivity establishes the internal stability of a certain community in the given region.

3.3.3 Existence of stability equilibrium

For the steady state equilibrium using Equation 6:

$$\frac{dS}{dt} = \frac{dV}{dt} = \frac{dI}{dt} = \frac{dR}{dt} = 0 \quad (6)$$

so we have Equations 7-9:

$$T - (1-r)\beta SI - rS - \mu_1 S = 0 \quad (7)$$

$$rS - (1-e)\beta VI - \mu_1 V = 0 \quad (8)$$

$$(1-r)\beta SI + (1-e)\beta VI - (\mu_1 + \mu_2 + \gamma)I = 0 \quad (9)$$

$$\gamma I - \mu_1 R = 0 \quad (10)$$

Solving simultaneously Equation 10 for the endemic equilibrium, we have Equations 11-13:

$$S^* = \frac{T}{(1-r)\beta I^* - (\mu_1 + r)} \quad (11)$$

$$V^* = \frac{rT}{[(1-r)\beta I^* - (\mu_1 + r)][(1-e)\beta I^* - \mu_1]} \quad (12)$$

$$R^* = \frac{\gamma I^*}{\mu_1} \quad (13)$$

3.3.4 Calculation of basic reproduction number

It is defined as the expected number of new nodes generated by indexed nodes during the whole of the susceptible nodes in the network.

Reproduction number without vaccination is $R_0 = \frac{T(1-r)\beta}{\mu_1(\mu_1+\mu_2+\gamma)}$, the reproduction number with vaccination is $R_0^V = \frac{T(1-r)\beta(\mu_1+(1-e)r)}{\mu_1(\mu_1+\mu_2+\gamma)(\mu_1+r)}$.

This threshold number or basic reproduction number depends on each of the infectious diseases of COVID-19. This will determine whether the virus is removed or stays in the given community. Thus, $R^V{}_0 < R_0$ will reduce the disease. The COVID-19 disease will be eliminated from the Community.

3.4 Equilibrium points

3.4.1 Infection-free equilibrium

The infection-free equilibrium is locally asymptotically stable if $R_0^V \le 1$. And also, it is unstable when $R_0^V > 1$.

Proof:

Linearization of the system of Equations 7-10 around the infection-free equilibrium J(1,0,0), we get the Jacobian matrix Equation 14:

$$J_{IFE} = \begin{pmatrix} -(\mu_1 + r) & 0 & -(1-r)\beta \\ r & -\mu_1 & 0 \\ 0 & 0 & -(\mu_1 + \mu_2 + \gamma) \end{pmatrix} \quad (14)$$

The characteristic equation is Equation 15:

$$[\lambda 1 + (\mu_1 + r)][(\lambda 2 + \mu_1)(\lambda 3 + (\mu_1 + \mu_2 + \gamma))] = 0 \quad (15)$$

where the eigen values are $\lambda 1 = -(\mu_1 + r)$, $\lambda 2 = -\mu_1$, $\lambda 3 = -(\mu_1 + \mu_2 + \gamma)$

Since all the eigenvalues are negative, the infection-free equilibrium is locally asymptotically stable.

Since all eigenvalues of the Jacobian matrix are strictly negative, the infection-free equilibrium (IFE) is locally asymptotically stable, and the endemic equilibrium is unstable. Thus, COVID-19 cannot invade the population.

3.4.2 Endemic equilibrium

Theorem: The endemic equilibrium is locally asymptotically stable in the region Ω if $R_0^V > 1$

Proof:

Proceeding similarly linearized the endemic equilibrium$J(S^*, V^*, I^*)$, we have Equation 16:

$$J_{EE} = \begin{pmatrix} -(1-r)\beta I^* - (r + \mu_1) & 0 & -(1-r)\beta S^* \\ r & -(1-e)\beta I^* - \mu_1 & -(1-e)\beta V^* \\ 0 & (1-e)\beta I^* & (1-e)\beta V^* + (1-r)\beta I^* - (\mu_1 + \mu_2 + \gamma) \end{pmatrix} \quad (16)$$

The characteristic equation is in the form of a cubic polynomial (Equation 17):

$$\lambda^3 + A\lambda^2 + B\lambda + C = 0 \tag{17}$$

where

$$A = -\{-(1-r)\beta I^* - (r+\mu_1) + (-(1-e)\beta I^* - \mu_1) + (1 - e)\beta V^* + (1-r)\beta I^* - (\mu_1 + \mu_2 + \gamma)]$$

$$B = -[((1-e)\beta I^*)(-(1-e)\beta V^*) - (-(1-r)\beta I^* - (r + \mu_1))(-(1-e)\beta I^* - \mu_1)$$
$$-(-(1-r)\beta I^* - (r+\mu_1))((1-e)\beta V^* + (1-r)\beta I^* - (\mu_1 + \mu_2 + \gamma))$$
$$-(1-e)\beta V^* + (1-r)\beta I^* - (\mu_1 + \mu_2 + \gamma)(-(1-e)\beta I^* - \mu)\}$$

$$C = -\{(1-e)\beta V^* + (1-r)\beta I^* - (\mu_1 + \mu_2 + \gamma)(-(1 - e)\beta I^* - \mu)(-(1-r)\beta I^* - (r+\mu_1))$$
$$+(-(1-r)\beta I^* - (r+\mu_1))((1-e)\beta I^*)(-(1-e)\beta V^*) + r((1-e)\beta I^*)(-(1-r)\beta S^*)\}$$

and $AB > C$

Rouwth Hrouth's condition is stable. Thus, the endemic equilibrium is locally asymptotically stable.

Routh-Hurtwicz conditions are precise for determining the stability of a larger system. Therefore, this system is stable at the endemic equilibrium.

3.5 Global stability analysis for endemic equilibrium

We deal with the geometric approach developed in the global stability of endemic equilibrium. We start with a review of the geometric approach.

Consider the independent dynamical system $\frac{dx}{dt} = f(x)$, where $f: D \to R^n, D \subset R^n$ is an open-set $f \in C^1$,. Let us consider the hypothesis that holds good.

(H_1) Ω is a simply connected set.

(H_2) It is a compact absorbing set $K \in \Omega$

(H_3) A unique equilibrium x exists in the system of differential Equations 1-4 in the region Ω.

Lemma: when the two hypotheses H_2 and H_3 satisfy the Bandixson condition in the C^1 of f(x) for all non-equilibrium points on system (1). If x_* is stable, then it is globally stable in the domain D.

Let $X \to p(x) \in \binom{n}{2} X \binom{n}{2}$ be a matrix-valued function C^1 for $x \in D$. Assume that $p^{-1}(x)$ exists and is continuous for $x \in K$. Define q using Equation 18:

$$q = \lim_{t\to\infty} \sup \sup_{x_0 \in K} \frac{1}{t} \int_0^t \mu(B(x(s, x_0))\, ds \tag{18}$$

where block matrix $B = p_f p^{-1} + pj^{[2]}p^{-1}$ .Thus, p_f is a matrix given by $(p_{ij}(x))_f = \left(\frac{\partial p_{ij}(x)}{\partial x}\right)^T f(x) = \nabla p_{ij}(x) f(x)$ and $j^{[2]}$ is second additive compounded matrix of Jacobian matrix J. While $\mu(B)$ is Lozinski measure of B with respect to the norm in R^n, $N = C_n^2$ and defined as $\mu(B) = \lim_{h\to 0} \frac{|I - hB| - 1}{h}$. This result proves the global stability of the endemic equilibrium.

3.6 Theorem

The unique endemic equilibrium point is globally stable in the region if $R_0{}^V > 1$ (Equation 19).

$$J = \begin{pmatrix} -(1-r)\beta I - (r+\mu_1) & 0 & -(1-r)\beta S \\ r & -(1-e)\beta I - \mu_1 & -(1-e)\beta V \\ 0 & (1-e)\beta I & (1-e)\beta V + (1-r)\beta I - (\mu_1 + \mu_2 + \gamma) \end{pmatrix} \tag{19}$$

Using the second additive-compounded matrix in Equation 20:

$$J^{[2]} = \begin{pmatrix} -[(1-r)\beta I + r + 2\mu_1 + (1-e)\beta I] & -(1-e)\beta V & (1-r)\beta S \\ (1-e)\beta I & -[(1-r)\beta I + r + 2\mu_1 + \mu_2 + \gamma] + (1-e)\beta V + (1-r)\beta S & 0 \\ 0 & -r & (1-e)\beta V + (1-r)\beta S + (1-e)\beta I - (2\mu_1 + \mu_2 + \gamma) \end{pmatrix} \tag{20}$$

Let us define the function

$$p(x) = (S, V, I) = diag\left\{1, \frac{I}{V}, \frac{I}{V}\right\} = \begin{pmatrix} 1 & 0 & 0 \\ 0 & \frac{I}{V} & 0 \\ 0 & 0 & \frac{I}{V} \end{pmatrix}$$

Then

$$p_f p^{-1} = diag\left\{0, \frac{I^1}{I} - \frac{V^1}{V}, \frac{I^1}{I} - \frac{V^1}{V}\right\} = \begin{pmatrix} 0 & 0 & 0 \\ 0 & \frac{I^1}{I} - \frac{V^1}{V} & 0 \\ 0 & 0 & \frac{I^1}{I} - \frac{V^1}{V} \end{pmatrix}$$

And

$$pJ^{[2]}p^{-1} = \begin{pmatrix} -[(1-r)\beta I + r + 2\mu_1 + (1-e)\beta I] & -(1-e)\beta V\left(\frac{V}{I}\right) & (1-r)\beta S\left(\frac{V}{I}\right) \\ (1-e)\beta I\left(\frac{I}{V}\right) & -[(1-r)\beta I + r + 2\mu_1 + \mu_2 + \gamma] + (1-e)\beta V + (1-r)\beta S & 0 \\ 0 & -r & (1-e)\beta V + (1-r)\beta S + (1-e)\beta I - (2\mu_1 + \mu_2 + \gamma) \end{pmatrix}$$

Also, $p_f p^{-1} + pj^{[2]}p^{-1} =$

$$\begin{pmatrix} -[(1-r)\beta I + r + 2\mu_1 + (1-e)\beta I] & -(1-e)\beta V\left(\frac{V}{I}\right) & (1-r)\beta S\left(\frac{V}{I}\right) \\ (1-e)\beta I\left(\frac{I}{V}\right) & -[(1-r)\beta I + r + 2\mu_1 + \mu_2 + \gamma] + (1-e)\beta V + (1-r)\beta S + \frac{I^1}{I} - \frac{V^1}{V} & 0 \\ 0 & -r & \frac{I^1}{I} - \frac{V^1}{V} + (1-e)\beta V + (1-r)\beta S + (1-e)\beta I - (2\mu_1 + \mu_2 + \gamma) \end{pmatrix}$$

Define the block matrix

$$B = p_f p^{-1} + pj^{[2]}p^{-1} = \begin{pmatrix} B_{11} & B_{12} \\ B_{21} & B_{22} \end{pmatrix}$$

where

$$B_{11} = (-[(1-r)\beta I + r + 2\mu_1 + (1-e)\beta I])$$

$$B_{12} = \left(-(1-e)\beta V\left(\frac{V}{I}\right) \quad (1-r)\beta S\left(\frac{V}{I}\right)\right)$$

$$B_{21} = \begin{pmatrix} (1-e)\beta I\left(\frac{I}{V}\right) \\ 0 \end{pmatrix}$$

$$\boldsymbol{B_{22}} = \begin{pmatrix} -[(\mathbf{1}-\boldsymbol{r})\boldsymbol{\beta I} + \boldsymbol{r} + \mathbf{2}\boldsymbol{\mu_1} + \boldsymbol{\mu_2} + \boldsymbol{\gamma}] + (\mathbf{1}-\boldsymbol{e})\boldsymbol{\beta V} + (\mathbf{1}-\boldsymbol{r})\boldsymbol{\beta S} + \frac{\boldsymbol{I^1}}{\boldsymbol{I}} - \frac{\boldsymbol{V^1}}{\boldsymbol{V}} & \mathbf{0} \\ -\boldsymbol{r} & \frac{\boldsymbol{I^1}}{\boldsymbol{I}} - \frac{\boldsymbol{V^1}}{\boldsymbol{V}} + (\mathbf{1}-\boldsymbol{e})\boldsymbol{\beta V} + (\mathbf{1}-\boldsymbol{r})\boldsymbol{\beta S} + (\mathbf{1}-\boldsymbol{e})\boldsymbol{\beta I} - (\mathbf{2}\boldsymbol{\mu_1} + \boldsymbol{\mu_2} + \boldsymbol{\gamma}) \end{pmatrix}$$

Next, for the vector norm and the Lodzinski measure for the norm, is followed by $\mu(B) \leq sup\{g_1, g_2\}$ where $g_1 = \mu(B_{11}) + |B_{12}|$ and $g_2 = |B_{21}| + \mu(B_{22})$, $|B_{12}|$ and $|B_{21}|$ are the matrix norms concerning the vector norm, and μ is the Lodzinski measure norm. We have Equations 21-24:

$$\mu(B_{11}) = (-[(1-r)\beta I + r + 2\mu_1 + (1-e)\beta I]) \quad (21)$$

$$|B_{12}| = -(1-e)\beta V\left(\frac{V}{I}\right) \quad (22)$$

$$|B_{21}| = (1-e)\beta I\left(\frac{I}{V}\right) \quad (23)$$

$$\mu(B_{22}) = max\{-[(1-r)\beta I + r + 2\mu_1 + \mu_2 + \gamma] + (1-e)\beta V + (1-r)\beta S + \frac{I^1}{I} - \frac{V^1}{V}, -r, \frac{I^1}{I} - \frac{V^1}{V} + (1-e)\beta V + (1-r)\beta S + (1-e)\beta I - (2\mu_1 + \mu_2 + \gamma)\} = -[(1-r)\beta I + r + 2\mu_1 + \mu_2 + \gamma] + (1-e)\beta V + (1-r)\beta S + \frac{I^1}{I} - \frac{V^1}{V} \quad (24)$$

These values can be substituted in g_1 and g_2, then we get Equations 25 and 26:

$$g_1 = \left(-[(1-r)\beta I + r + 2\mu_1 + (1-e)\beta I] + (-(1-e)\beta V)\left(\frac{V}{I}\right)\right) \leq \frac{I^1}{I} - \mu_1 \quad (25)$$

$$g_2 = (1-e)\beta I\left(\frac{I}{V}\right) - [(1-r)\beta I + r + 2\mu_1 + \mu_2 + \gamma] + (1-e)\beta V + (1-r)\beta S + \frac{I^1}{I} - \frac{V^1}{V} \leq \frac{I^1}{I} - \mu_1 \mu(B) \leq sup\{g_1, g_2\} \leq \frac{I^1}{I} - \mu_1 \quad (26)$$

Along each solution $(S(t), V(t), I(t))$ of the system of Equations 1-4 $(S(0), V(0), I(0)) \in K$, where K is an absorbing compact set. We have Equation 27:

$$\frac{1}{t}\int_0^t \mu(B)\, ds \leq \frac{1}{t}\left(\frac{I^1}{I} - \mu_1\right) ds = \frac{1}{t} ln \frac{I(t)}{I(0)} - \mu_1$$

$$\Rightarrow q = \lim_{t\to\infty} sup \sup_{x_0 \in K} \frac{1}{t}\int_0^t \mu(B(x,(s,x_0)))\, ds$$

$$\leq sup \sup_{x_0 \in K} \frac{1}{t} ln \frac{I(t)}{I(0)} - \mu_1 < 0 \quad (27)$$

As a result, the endemic equilibrium is globally stable in the region **Ω**.

In this case, there is no periodic solution or homoclinic orbit / heteroclinic cycle, and it is an artifact of the method. This proves to establish the limit cycle that lies in the community, and there are no holes / critical points in the given community. Therefore, the pandemic has become endemic. This result suggests that the endemic equilibrium is globally stable even though 'e' is much larger than μ_1.

4. Failure mode and effects analysis of the vaccination process

In addition to the proposed SVIR model, the failure mode and effect analysis (FMEA) approach is used to evaluate the efficiency of the vaccination process. It is a very influential method utilized in industries to analyze failure modes and their effects on systems/processes. Initially, it was developed in the aeronautics field, but these days, it is also extensively used in the medical sector. Koucha and Yang (2021) carried out the Bayesian risk assessment of COVID-19 using the SEIR model and FMEA methodology.[20] Lateef *et al.* (2020) conducted a study to propose infection control measures using FMEA during COVID-19.[21] Latt *et al.* (2021) conducted FMEA to develop a technique for preventing the risk of SARS-CoV-2 infection in a retrocession unit.[22] The FMEA analysis is carried out at three levels, namely design, system, and process level. It is a vast process performed in six steps: define the process, set standard rules, define the process in blocks, identify failure modes and their effects, find the critical items list, and prepare the document for analysis. It prioritizes the discovered failure modes using occurrence and severity ranking. The assessment is made using the risk priority number (RPN) method, whose value varies between 1 and 1000 as severity, occurrence, and detection ranking lie between 1 and 10. The ranking criteria for severity, detection, and occurrence are given in Tables 2-4.[23]

Table 2: Ranking of failure detection.

S. No.	Chance of detection	Rank meaning	Ranking
1	Almost certain	Influential weak points in the process will almost certainly be detected	1,2
2	High	Good chance of detection of weakness in the process	3,4
3	Mild	Possibility to detect weakness in the process	5,6
4	Low	Influential weak points in the process will be difficult to detect	7,8
5	Very low	Influential weak points in the process will probably not be difficult to detect	9
6	Remote/almost uncertain	Influential weak points in the process cannot be detected	10

Table 3: Ranking of failure occurrence.

S. No.	Ranking term	Description of the ranking term	Occurrence probability	Rank
1	almost uncertain/remote	Rarely any failure occur	Less than 1 in 1000000	1
2	Low	Expectation of failure is very low	1 in 20000	2
			1 in 4000	3
3	Mild	Occasionally any failure occurs	1 in 1000	4
			1 in 400	5
			1 in 80	6
4	High	Failure occurs in repetition	1 in 40	7
			1 in 20	8
5	Very high	Failure occurrence is inevitable	1 in 8	9
			1 in 2	10

Table 4: Ranking of severity of the failure mode and effect.

S. No.	Severity of failure mode	Description of severity category	Rank
1	Insignificant	No serious consequences due to failure of the system	1
2	Low	Cause a slight displeasure in customers	2, 3
3	Mild	Resulted in dissatisfaction among a few customers	4, 5, 6
4	High	High degree of dissatisfaction, but no violation of the rule frames by regulatory bodies and safety	7, 8
5	Very high	Compromise operational safety involves in violating of rules	9, 10

Table 5: FMEA of vaccination process.

Process function	Key failure mode	Effect of failure	S.	Key cause of failure	O.	D.	RPN	Recommended actions
Vaccine availability	Low Availability	Delays in vaccination, increase the chances of infection and create a black market for vaccines	9	Bureaucracy	9	10	810	Simplify ordering procedure
	Delay at production plant		9	The supplier is away/downtime	9	9	729	Establish new plants at different geographical locations and give permission to other pharma companies for production
	Late delivery		9	Constraints in terms of raw material availability and international agreements to supply	8	6	432	Explore new options for raw material and give priority to inhouse supply

Process function	Key failure mode	Effect of failure	S.	Key cause of failure	O.	D.	RPN	Recommended actions
	Order not placed by Government in advance		9	Economic factors and government limitations	9	5	405	Give priority to vaccines over other non-essential projects
	Lack of Hospitals		9	Medical infrastructure not developed properly	8	10	720	Develop medical infrastructure and allow more private hospitals for vaccination
Medical Infrastructure & Staff availability	shortage of medical supplies like vials, syringes, etc.	Burden on hospitals, and pharma companies; stop production due to non-availability and chances of AEFI reporting increase	9	Non-availability of raw materials and no communication with the manufacturer	9	10	810	Promote new manufacturers to develop medical supplies
	Lack of specialized medical doctors and nurses		10	Less number of trained personnel due to the existing limited number of medical seats	9	10	900	Increase the seats of medical personnel and train the paramedical staff
Supply Chain	Lack of transport facility with suitable equipment's like deep freezers to transport vaccine	Vaccine cannot be stored and transported	10	Supply chain infrastructure not properly developed	8	8	640	Develop a sufficient transportation facility
Storage Facility	Lack of Deep freezers in government hospitals situated in rural and remote areas	Wastage of vaccine	10	Advanced equipment not available	8	7	560	Develop storage facilities either by manufacturing or importing from other countries
	Trust invaccines and vaccines not available for all	People do not come to medical centers for vaccination	8	Children < 18 years old cannot be vaccinated and that is a very sensitive portion of the population that can be infected	7	7	392	Develop vaccines for children as well as develop proper mechanisms for vaccination so that minimum wastage resulted
Societal Beliefs	Anti-vaccine campaign	Some political parties run campaigns against vaccination	6	Some persons exposed to COVID-19, even after taking the vaccine develop untrust and	5	4	120	Create faith in vaccines through advertisement

Process function	Key failure mode	Effect of failure	S.	Key cause of failure	O.	D.	RPN	Recommended actions
				help in the growing anti-vaccine campaign				
Government Policies	Fails to develop trust and environment for vaccination	Not even the distribution of vaccines it resulted in fear of the spread of COVID-19 and failure of vaccination	6	Due to political, external, internal, and economic reasons	6	2	72	The government in an unbiased way and sets an example to the public so that the population comes for vaccination

5. Data analysis

In this section, we have taken into consideration the COVID-19 vaccines available (WHO-approved data) with the efficacy of the vaccines by Patel *et.al*, COVID-19 vaccine efficacy summary of the Institute for Health Metrics and Evaluation in Feb 2021.[24] The study showcases the efficacy of all vaccines with the data from the trials done on each vaccine in various age groups. The study is very helpful in defining the immunity of the population and the period for which this immunity will be sustained in various age groups.

This study will define the Susceptibility of the total population and the population that is still exposed to this virus. The study shown below showcases a study that defines the decay in immunity of the population with time, which increases the probability of the population being infected again because of the low efficacy of the vaccines. The study is carried out based on WHO COVID-19 vaccination data available for various countries. Table 5 shows the failure mode and effect analysis of vaccines, while Tables 6-8 show the study of the efficacy of the listed vaccines.

Table 6: Vaccine efficacy.

Effectiveness at preventing	Ancestral		Alpha		Beta		Gamma		Delta		Omicron	
Vaccine	Severe diseases %	Infection %	Severe diseases %	Infection %	Severe diseases %	Infection %	Severe diseases %	Infection %	Severe diseases %	Infection %	Severe diseases %	Infection %
AstraZeneca	94	63	94	63	94	69	94	69	94	69	71	36
CanSina	66	62	66	62	64	61	64	61	64	61	48	32
Coronavac	50	47	50	47	49	46	49	46	49	46	37	24
Covaxin	78	73	78	73	76	72	76	72	76	72	57	38
Johnson	86	72	86	72	76	64	76	64	76	64	57	33
Moderna	97	92	97	92	97	91	97	91	97	91	73	48
Novavax	89	83	89	83	86	82	86	82	86	82	65	43
Pfizer	95	86	95	86	95	84	95	84	95	84	72	49
Sinapharm	73	68	73	68	71	67	71	67	71	67	53	35
Sputnik-V	92	86	92	86	89	85	85	89	89	85	67	49
Other Vaccines	75	70	75	70	73	69	73	69	73	69	55	36
Other Vaccines	91	86	91	86	88	85	88	85	88	85	67	45

Table 7: Vaccine efficacy.

Vaccine_name	Product_name	Company_name
Anhui ZL - Zifivax	Zifivax	Anhui Zhifei Longcom Biopharmaceutical
AstraZeneca - AZD1222	AZD1222	AstraZeneca
AstraZeneca - Vaxzevria	Vaxzevria	AstraZeneca
Beijing CNBG - BBIBP-CorV	BBIBP-CorV	Beijing Bio-Institute Biological Products (CNBG)
Bharat - Covaxin	Covaxin	Bharat Biotech
CanSino - Convidecia	Convidecia	CanSino Biologicals
CIGB - CIGB-66	CIGB-66	Center for Genetic Engineering and Biotechnology
Gamaleya - Sputnik-Light	Sputnik-Light	Gamaleya Research Institute
Gamaleya - Gam-Covid-Vac	Gam-Covid-Vac	Gamaleya Research Institute
IMB - Covidful	Covidful	Insitute of Medical Biology
Finlay - Soberana Plus	Soberana Plus	Instituto Finlay de Vacunas
Finlay - Soberana-02	Soberana-02	Instituto Finlay de Vacunas
Janssen - Ad26.COV 2-S	Ad26.COV 2-S	Janssen Pharmaceuticals
Moderna - mRNA-1273	mRNA-1273	Moderna
Moderna - Spikevax	Spikevax	Moderna
Novavax-NUVAXOVID	NUVAXOVID	Novavax
Pfizer BioNTech - Comirnaty	Comirnaty	Pfizer BioNTech
RIBSP - QazVac	QazVac	Research Institute for Biological Safety Problems
SII - Covishield	Covishield	Serum Institute of India
Shenzhen - LV-SMENP-DC	LV-SMENP-DC	Shenzhen Geno Immune Medical Institute
Sinovac - CoronaVac	Coronavac	Sinovac
SRCVB - EpiVacCorona	EpiVacCorona	State Research Centre of Virology & Biotechnology
Wuhan CNBG - Inactivated	Inactivated SARS-CoV-2 vaccine	Wuhan Institute of Biological Products (CNBG)
Zydus - ZyCov-D	ZyCov-D	Zydus Cadila

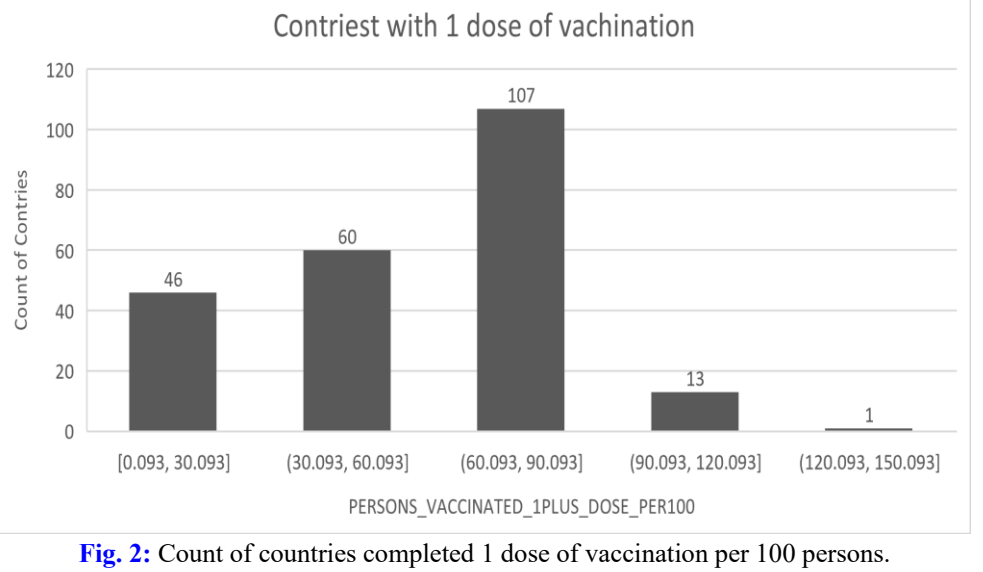

Fig. 2: Count of countries completed 1 dose of vaccination per 100 persons.

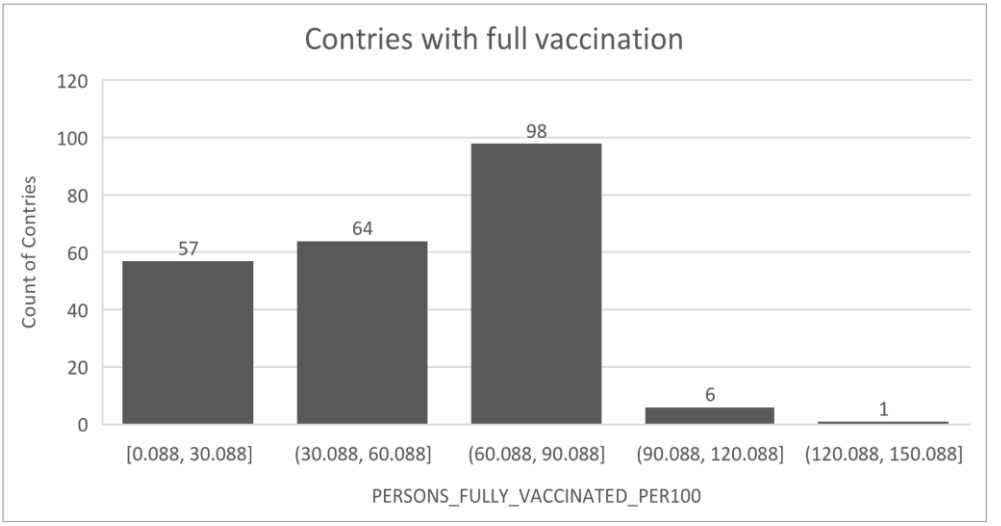

Fig. 3: Count of countries completed full dose of vaccination per 100 persons.

Table 8: Efficacy and the corresponding company name.

Company_name	Efficacy
CanSino biologicals	66
Sinovac	73
Bharat biotech	78
Novavax	89
Gamaleya research institute	92
AstraZeneca	94
Moderna	97

Figs. 2 and 3 show that the majority of countries lack in completing at least one dose of vaccination. As shown in Fig. 2, out of 228 countries listed by WHO, only 106 can complete a good ratio of 1 dose of vaccination, whereas other countries still struggle to achieve this aim. Similarly, Fig. 3 shows that only a few countries can fulfill the double dose of the vaccine to their population, which leaves the majority of the population exposed to the virus over time, with decay in immunity raised by vaccines.

This leaves the big question in two directions: the exposure of the virus to the unvaccinated population and the exposure of the virus to the vaccinated population over time due to the low efficacy of the vaccine. To identify the risk and time required to get the majority of the population vaccinated, this study is performed using the SIR Epidemic Model to estimate the percentage of the exposed and susceptible population that is open to the next variant of COVID-19. As shown in the proposed section, the SIR model is shown with various inputs.

Fig. 4 shows a study of the spread of the COVID-19 virus and its peak in the first wave, taking into consideration WHO data for India, where beta and gamma are 0.3 and 1/10, respectively, and the number of infected population every 100 people is taken into consideration. However, the result is incomplete because the first wave was avoided by social distancing and medical treatment, not by vaccination. The figure also shows that even though the infection was reduced in the susceptible population, it is still high, which is prone to infection. This study shows the role of vaccination using the SVIR mode. Fig. 4 shows the prediction of the SEIR Model for the spread of COVID-19. The infection rate, which is spread from one to another, is 10 in one day, represented by beta, beta = 0.1588, sigma = 0.1566, gamma = 0.0136.

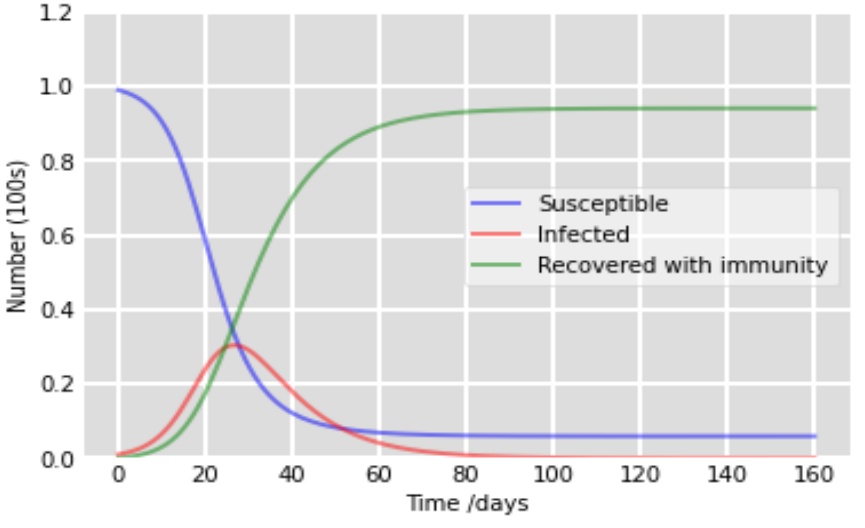

Fig. 4: SIR model to estimate the effect of the first wave of COVID-19 and its peak every 100 persons.

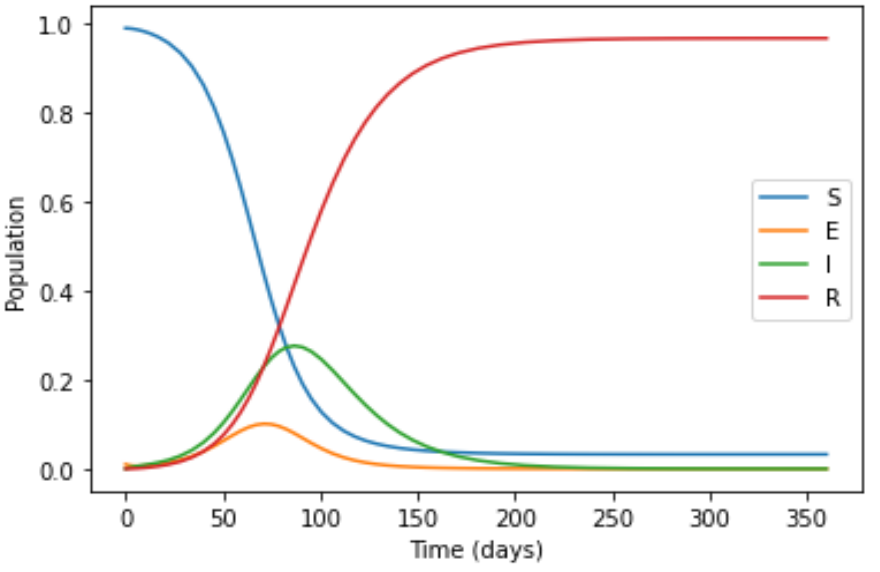

Fig. 5: Basic SEIR model to estimate the effect of COVID-19 spread.

Fig. 5 shows the outcome of the proposed SEIR model, which shows the susceptible, exposed, infected, and recovered population in China. In the availability of the vaccination process, the behavior of the model SVIR (susceptible, vaccinated, infected, and recovered) population is shown in Fig. 6, which shows that even after vaccination, 17 % of the total population remains susceptible after vaccination and exposure to the virus. This data does not include the population that is not vaccinated to date; this data is only about the vaccinated people who are still exposed to the virus. The outcome of total vaccination data available for 635 days, where the rate of vaccination was 35.8% over every 100 people for the first dose of vaccination, is depicted in Fig. 7. The sample includes eight types of vaccination in China, with an average of 88.5% efficacy.

Fig. 8 shows the countries with high vaccination rates for first doses of vaccination. In this study, these countries are taken into consideration. A similar study was done for India, which shows that vaccination took nearly 200 days to vaccinate the majority of the population, out of which nearly 60% of the population got vaccinated, leaving 40% of the population exposed to the virus. Fig. 8 also showcased that even after vaccination, nearly 20% of the population is still susceptible to the virus due to the low efficacy of the vaccine used.

Fig. 9 shows that after the first dose of the vaccination, the immunity of a person is high for 40 days, and then the immunity degrades, which makes the person exposed and susceptible to the virus, depending upon their own immunity rather than immunity due to vaccination. This can only be improved with second doses of the vaccine. In India, the percentage of the population getting a second dose is very low.

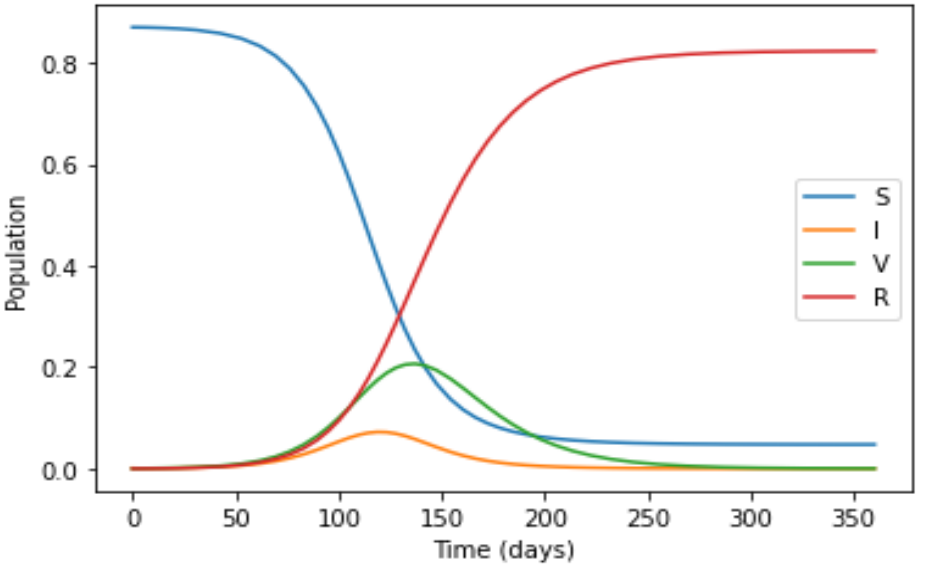

Fig. 6: Proposed SVIR model to estimate the effect of vaccination and its efficacy.

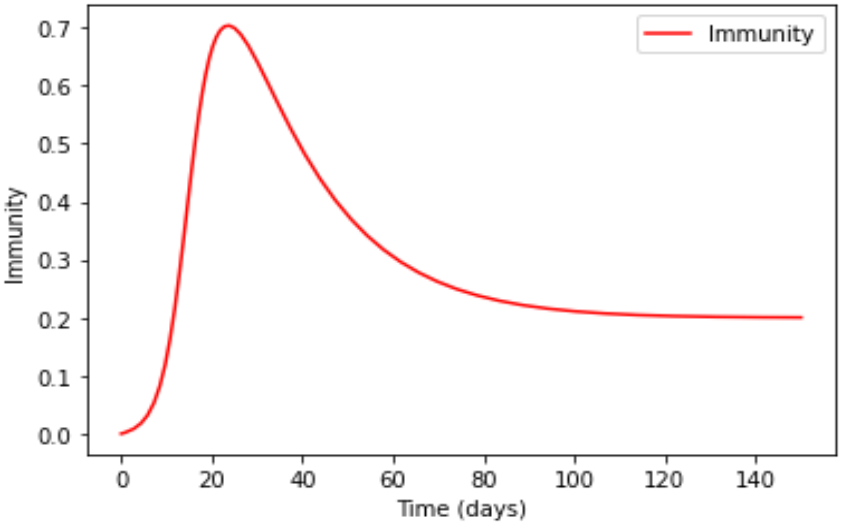

Fig. 7: Change in immunity after the first vaccination dose for China.

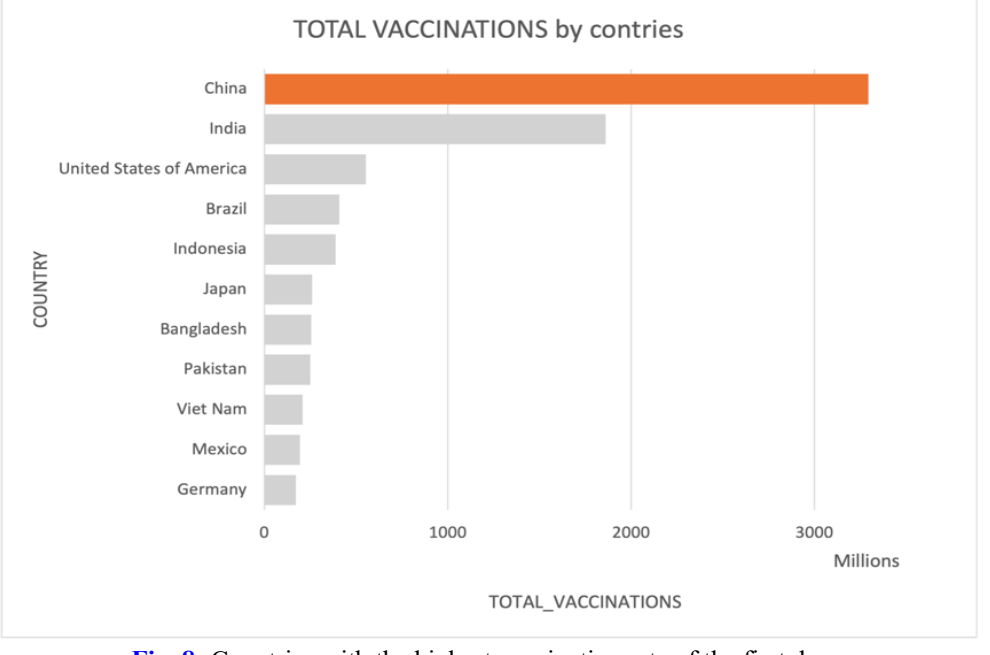

Fig. 8: Countries with the highest vaccination rate of the first dose.

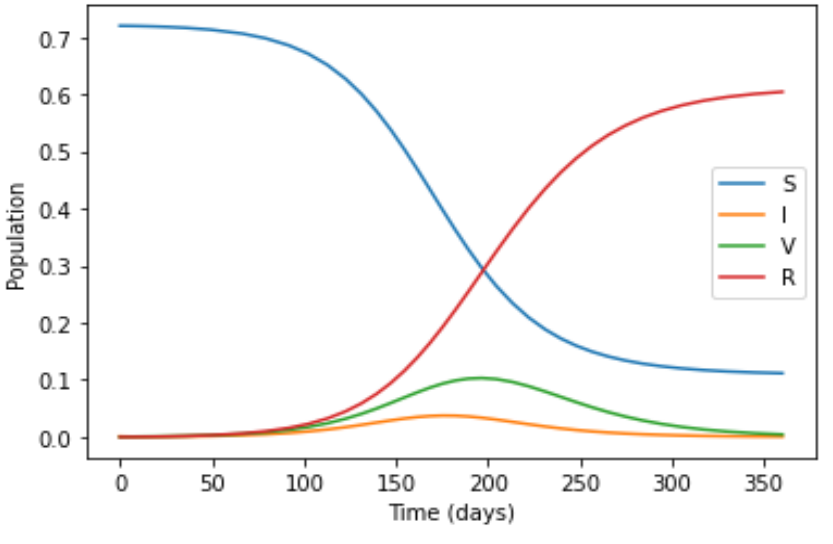

Fig. 9: Study for immunity in India after vaccination.

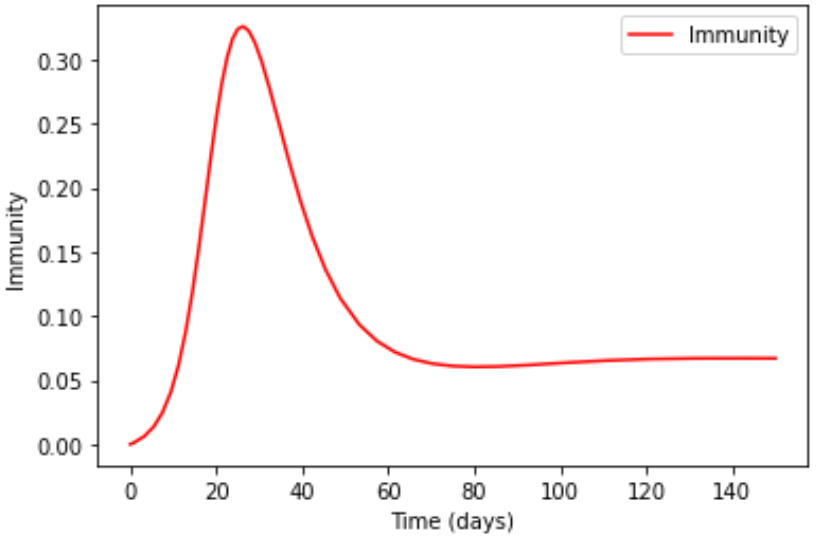

Fig. 10: Study for immunity in the United States due to the vaccine.

A similar study was done in the United States as shown in Fig. 10. The model shows a low vaccination rate and only 65% of the population participating in the vaccination process with 20% of that remaining susceptible to the virus due to the low efficacy of the vaccines which leaves the population that is not vaccinated and the population with low immunity due to low efficacy open and exposed to the virus. This situation will lead to the spread of the virus in the continuity of the second and third waves of the modified COVID-19 virus. This makes this pandemic a growing chain of vaccination drives to improve immunity among the population.

Fig. 11 also supports the above discussion, where in the United States, 5 types of vaccines were used with low efficacy, which improved the immunity only for nearly 35-40 days and then brought the vaccinated person into the category of susceptibility. This means the single does prevent the person for 40-55 days, and then the second dose becomes available in India. It is preferable to support the immune system, as shown in Fig. 12.

6. Conclusion

In this work, a study on the efficacy of vaccines is conducted to observe the change in immunity of the population after vaccination. Vaccination plays an important role in any pandemic, COVID-19 or any other pandemic, but vaccines with low efficacy reduce the chances of eradicating the virus. This allows the virus to propagate and evolve into new variants. This study shows the vaccination process in various countries with the type of vaccine used and the total population vaccinated with at least one dose. These parameters define the percentage of the population still exposed to the virus and the population that is immune in the current situation, which may be exposed in the future due to the low efficacy of the vaccine. As shown in the result section, the proposed SVIR model can predict the immunity of a vaccinated person with the time at which the person will be exposed to the virus with

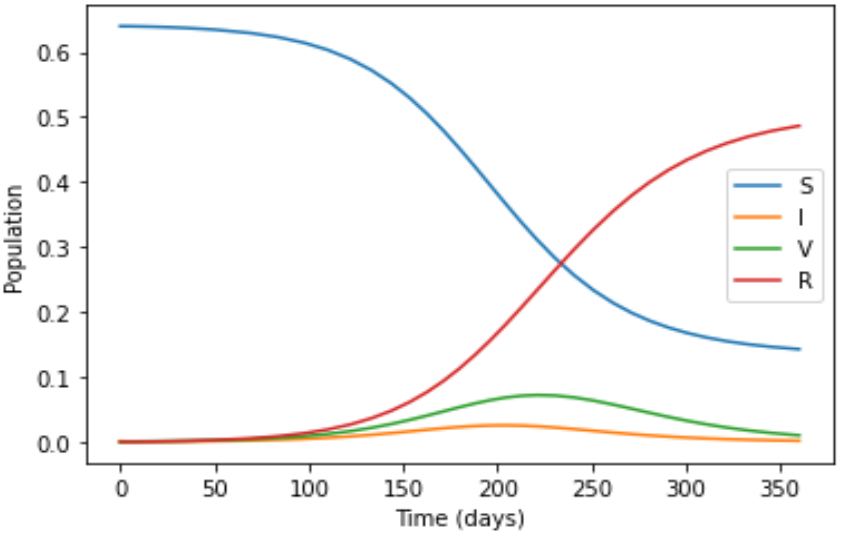

Fig. 11: Study for immunity in the United States after vaccination.

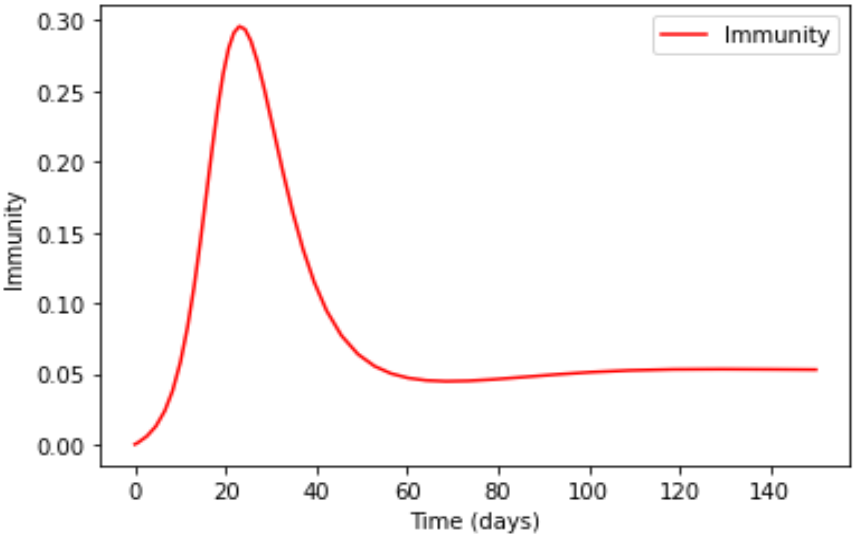

Fig. 12: Study for immunity in India due to the vaccine.

low immunity. This is why the second dose of the vaccine is brought into the picture to increase the effectiveness of the first dose. The vaccines with two doses showcase low efficacy, whereas the vaccine with high effectiveness does not need a second dose. The study can further be done on the time frame of the next wave and the count of the population that will be exposed to the future variants of the COVID-19 virus.

Conflict of Interest

There is no conflict of interest.

Supporting Information

Not applicable.

References

[1] G. Pinter, I. Felde, A. Mosavi, P. Ghamisi, R. Gloaguen, COVID-19 pandemic prediction for Hungary; A hybrid machine learning approach, *Mathematics*, 2020, **8**, 890, doi: 10.3390/math8060890.

[2] A. Singhal, P. Singh, B. Lall, S. D. Joshi, Modeling and prediction of COVID-19 pandemic using Gaussian mixture model, *Chaos, Solitons & Fractals*, 2020, **138**, 110023, doi: 10.1016/j.chaos.2020.110023.

[3] A. Kumar, P. K. Gupta, A. Srivastava, A review of modern technologies for tackling COVID-19 pandemic, *Diabetes & Metabolic Syndrome: Clinical Research and Reviews*, 2020, **14**, 569-573, doi: 10.1016/j.dsx.2020.05.008.

[4] S. Wang, B. Kang, J. Ma, X. Zeng, M. Xiao, J. Guo, M. Cai, J. Yang, Y. Li, X. Meng, B. Xu, A deep learning algorithm using CT images to screen for Corona virus disease (COVID-19), *European Radiology*, 2021, **31**, 6096-6104, doi: 10.1007/s00330-021-07715-1.

[5] A. Narin, C. Kaya, Z. Pamuk, Automatic detection of coronavirus disease (COVID-19) using X-ray images and deep convolutional neural networks, *Pattern Analysis and Applications*, 2021, **24**, 1207-1220, doi: 10.1007/s10044-021-00984-y.

[6] L. Wang, Z. Q. Lin, A. Wong, COVID-Net: a tailored deep convolutional neural network design for detection of COVID-19 cases from chest X-ray images, *Scientific Reports*, 2020, **10**, 19549, doi: 10.1038/s41598-020-76550-z.

[7] Y. Koucha, Q. Yang, A Bayesian risk assessment of the COVID-19 pandemic using FMEA and a modified SEIR epidemic model, *International Journal of Metrology and Quality Engineering*, 2021, **12**, 14, doi: 10.1051/ijmqe/2021012.

[8] X. Xu, X. Jiang, C. Ma, P. Du, X. Li, S. Lv, L. Yu, Q. Ni, Y. Chen, J. Su, G. Lang, Y. Li, H. Zhao, J. Liu, K. Xu, L. Ruan, J. Sheng, Y. Qiu, W. Wu, T. Liang, L. Li, A deep learning system to screen novel coronavirus disease 2019 pneumonia, *Engineering*, 2020, **6**, 1122-1129, doi: 10.1016/j.eng.2020.04.010.

[9] S. Rath, A. Tripathy, A. R. Tripathy, Prediction of new active cases of coronavirus disease (COVID-19) pandemic using multiple linear regression model, *Diabetes & Metabolic Syndrome: Clinical Research & Reviews*, 2020, **14**, 1467-1474, doi: 10.1016/j.dsx.2020.07.045.

[10] I. Rahimi, F. Chen, A. H. Gandomi, A review on COVID-19 forecasting models, *Neural Computing and Applications*, 2023, **35**, 23671-23681, doi: 10.1007/s00521-020-05626-8.

[11] I. Rahimi, A. H. Gandomi, P. G. Asteris, F. Chen, Analysis and prediction of COVID-19 using SIR, SEIQR, and machine learning models: Australia, Italy, and UK cases, *Information*, 2021, **12**, 109, doi: 10.3390/info12030109.

[12] A. S. Ahmar, E. B. del Val, Sutte, ARIMA: short-term forecasting method, a case: covid-19 and stock market in Spain, *Science of the Total Environment*, 2020, **729**, 138883, doi: 10.1016/j.scitotenv.2020.138883.

[13] M. A. A. Al-qaness, A. A. Ewees, H. Fan, M. Abd El Aziz, Optimization method for forecasting confirmed cases of COVID-19 in China, *Journal of Clinical Medicine*, 2020, **9**, 674, doi: 10.3390/jcm9030674.

[14] N. Chintalapudi, G. Battineni, F. Amenta, COVID-19 virus outbreak forecasting of registered and recovered cases after sixty day lockdown in Italy: A data driven model approach, *Journal of*

Microbiology, Immunology and Infection, 2020, **53**, 396-403, doi: 10.1016/j.jmii.2020.04.004.
[15] L. Moftakhar, S. Mozhgan, M. S. Safe, Exponentially increasing trend of infected patients with COVID-19 in Iran: a comparison of neural network and ARIMA forecasting models, *Iranian Journal of Public Health*, 2020, **49**, 92-100, doi: 10.18502/ijph.v49iS1.3675.
[16] R. M. Chaudhry, A. Hanif, M. Chaudhary, S. Minhas, K. Mirza, T. Asif, S. A. Gilani, M. Kashif, Coronavirus disease 2019 (COVID-19): forecast of an emerging urgency in Pakistan, *Cureus*, 2020 **12**, 1-15, doi: 10.7759/cureus.8346
[17] D. Chen, X. Chen, J. Chen, Reconstructing and forecasting the COVID-19 epidemic in the United States using a 5-parameter logistic growth model, *Global Health Research and Policy*, 2020, **5**, 25, doi: 10.1186/s41256-020-00152-5.
[18] V. K. R. Chimmula, L. Zhang, Time series forecasting of COVID-19 transmission in Canada using LSTM networks, *Chaos, Solitons and Fractals*, 2020, **135**, 109864, doi: 10.1016/j.chaos.2020.109864.
[19] G. C. Calafiore, C. Novara, C. Possieri, A time-varying SIRD model for the COVID-19 contagion in Italy, *Annual Reviews in Control*, 2020, **50**, 361-372, doi: 10.1016/j.arcontrol.2020.10.005.
[20] L. Yan, H. Zhang, J. Goncalves, Y. Xiao, M. Wang, Y. Guo, C. Sun, X. Tang, L. Jin, M. Zhang, X. Huang, Y. Xiao, H. Cao, Y. Chen, T. Ren, F. Wang, Y. Xiao, S. Huang, X. Tan, N. Huang, B. Jiao, Y. Zhang, A. Luo, L. Mombaerts, J. Jin, Z. Cao, S. Li, H. Xu, A machine learning-based model for survival prediction in patients with severe COVID-19 infection, *medRxiv*, 2020, 1-25, doi: 10.1101/2020.02.27.20028027.
[21] F. Lateef, S. Stawicki, L. Xin, S. Krishnan, A. Sanjan, F. Sirur, J. Balakrishnan, R. Goncalves, S. Galwankar, Infection control measures, *in situ* simulation, and failure modes and effect analysis to fine-tune change management during COVID-19, *Journal of Emergencies, Trauma, and Shock*, 2020, **13**, 239, doi: 10.4103/jets.jets_119_20.
[22] E. E. V. Latt, Y. Moutaouakkil, Z. Qriouet, Y. Atbib, Y. Tadlaoui, J. Lamsaouri, Y. Bousliman, Failure mode and effect analysis: a technique to prevent the risk of SARS-COV-2 infectionin A retrocession unit, *Indian Journal of Forensic Medicine and Toxicology*, 2021, **15**, 2878, doi: 10.37506/ijfmt.v15i3.15742.
[23] B. S. Dhillon, Maintainability, maintenance, and reliability for engineers, Boca Raton, CRC Press, 2006, 200, ISBN: 9780429128219.
[24] M. K. Patel, I. Bergeri, J. S. Bresee, B. J. Cowling, N. S. Crowcroft, K. Fahmy, S. Hirve, G. Kang, M. A. Katz, C. F. Lanata, M. L'Azou Jackson, S. Joshi, M. Lipsitch, J. M. Mwenda, F. Nogareda, W. A. Orenstein, J. R. Ortiz, R. Pebody, S. J. Schrag, P. G. Smith, P. Srikantiah, L. Subissi, M. Valenciano, D. W. Vaughn, J. R. Verani, A. Wilder-Smith, D. R. Feikin, Evaluation of post-introduction COVID-19 vaccine effectiveness: summary of interim guidance of the World Health Organization, *Vaccine*, 2021, **39**, 4013-4024, doi: 10.1016/j.vaccine.2021.05.099.